SCIENCE CHINA
Earth Sciences

• RESEARCH PAPER •

June 2015 Vol.58 No.6: 1005–1017
doi: 10.1007/s11430-014-5016-z

Distinct distribution revealing multiple bacterial sources for 1-*O*-monoalkyl glycerol ethers in terrestrial and lake environments

YANG Huan[1*], ZHENG FengFeng[2], XIAO WenJie[1] & XIE ShuCheng[1]

[1] *State Key Laboratory of Biogeology and Environmental Geology, China University of Geosciences, Wuhan 430074, China;*
[2] *State Key Laboratory of Marine Geology, Tongji University, Shanghai 200092, China*

Received September 28, 2014; accepted November 28, 2014; published online January 29, 2015

The 1-*O*-monoalkyl glycerol ethers (MAGEs) were initially viewed as the biomarkers for sulfate-reducing bacteria (SRB) mediating anaerobic oxidation of methane in the marine environments. However, limited information is known about their distribution in terrestrial and other aquatic settings including soils, fresh water lakes, and cave sediments, which may obscure our understanding of their biological sources. Here we found that MAGEs were ubiquitous but differed obviously in distributional pattern among those environments. The surface soils are dominated generally by $i\mathrm{C}_{15:0}$-MAGE, followed by $n\mathrm{C}_{16:0}$-MAGE whereas the lake sediments show the opposite, resulting in significantly higher $i\mathrm{C}_{15:0}/n\mathrm{C}_{16:0}$ ratios in soils than in lake sediments. The cave deposits are characterized by considerably higher proportions of branched MAGEs than the former two environments. The logarithm of $i\mathrm{C}_{15:0}/a\mathrm{C}_{15:0}$ ratio shows a significant negative correlation with soil pH, likely reflecting an adaptation of microbial cell membrane to change in the ambient proton concentration. The MAGE profiles in cultured bacteria cannot fully explain the MAGE distribution in all the samples analyzed. Therefore, MAGEs in soil, lake sediments, and cave deposits likely have additional biological source(s) other than SRB and cultured MAGE-producing bacteria. The difference in MAGE pattern among environments is likely to be attributed to change in microbial communities.

1-*O*-monoalkyl glycerol ethers, soil, lake sediments, cave deposits, biological sources

Citation: Yang H, Zheng F F, Xiao W J, et al. 2015. Distinct distribution revealing multiple bacterial sources for 1-*O*-monoalkyl glycerol ethers in terrestrial and lake environments. Science China: Earth Sciences, 58: 1005−1017, doi: 10.1007/s11430-014-5016-z

The glycerol ether lipids (GEL) in natural environments exhibit a large structural diversity in the alkyl substituent. These compounds, including glycerol dialkyl glycerol tetraethers (GDGTs), dialkyl glycerol ethers (DAGEs), 1-*O*-monoalkyl glycerol ethers (MAGEs), and glycerol dialkanol diethers (GDDs), etc. have unique ether bonds that are more stable than ester and amide bonds in the diacylglycerol of eukaryotes and bacteria. The isoprenoidal GELs, e.g., archaeol, generally come from Archaea with 2,3-di-*O*-alkyl-*sn*-glycerol stereo-configuration whereas non-isoprenoidal GELs, like MAGEs and DAGEs, typically have bacterial sources with alkyl chain(s) bound to *sn*-1 and *sn*-2 positions of glycerol backbone (Weijers et al., 2006a). GELs were initially found primarily in marine hydrothermal vents (Bradley et al., 2009), cold seeps with anaerobic oxidation of methane (AOM) (Hinrichs et al., 2000; Pancost et al., 2001; Blumenberg et al., 2004), terrestrial hot springs (Jahnke et al., 2001), silica sinters (Pancost et al., 2005, 2006), and a natural CO_2 vent in soil (Oppermann et al., 2010). Later on, more studies show the ubiquity of some GELs including archaeal isoprenoid GDGTs (iGDGTs), bacterial branched GDGTs (bGDGTs), and their corresponding GDDs in the temperate environments, e.g., soils (Weijers et al., 2006b; Liu et al., 2012; Yang et al., 2014a), lakes (Pearson et al., 2011), and marine water columns

*Corresponding author (email: yhsailing@163.com)

© Science China Press and Springer-Verlag Berlin Heidelberg 2015

(Schouten et al., 2000). The earliest discovery of MAGEs and iGDGTs in marine sediments has been extended to the Middle Triassic (Saito et al., 2013) and Middle Jurassic (Jenkyns et al., 2012), respectively, reflecting the resistance of ether bond to degradation. The sensitivity of iGDGTs and bGDGTs to temperature allows them to be used as paleothermometers in marine and terrestrial environment, respectively (Schouten et al., 2002; Weijers et al., 2007).

The widespread recognition about MAGEs (Figure 1(a)) in sediments was often associated with AOM because MAGEs were considered as the biomarkers for sulfate-reducing bacteria (SRB) that work in syntrophy with methanotrophic archaea (Hinrichs et al., 2000; Pancost et al., 2001; Blumenberg et al., 2004). This can be supported by the strongly depleted $\delta^{13}C$ of MAGEs found in the AOM environments (Hinrichs et al., 2000; Orphan et al., 2001) as well as the occurrence of MAGEs in some SRB pure cultures, e.g., *Desulfosarcinales* (Rütters et al., 2001). Nevertheless, MAGEs have been also reported in sulfur-oxidizing *Aquifex* (Jahnke et al., 2001), denitrifying *Planctomycetes* (Sinninghe Damsté et al., 2004), and nitrate-reducing *Ammonifex degensii* (Huber et al., 1996), all of which are bacteria favoring anoxic and (or) high temperature habitats. Reasonably, Oppermann et al. (2010) found abundant MAGEs with a tremendous structural diversity in anoxic soils at a natural CO_2 vent. A recent study of marine suspended particulate organic matter and surface sediments shows that MAGEs are widespread in the marine water column and sediments, suggesting they likely originate from some unknown aerobic bacterial sources other than SRB in marine environments (Hernandez-Sanchez et al., 2014). In fact, MAGEs are probably the constituents of 1-*O*-alkyl-2, 3-diacyl-*sn*-glycerol, 1-*O*-alkyl-2-acyl-3-*sn*-glycero-phospholipids or structurally similar glycerolipids (e.g., plasmalogens; Řezanka et al., 2012) because MAGEs can be detected only in the samples subjected to saponification or acid hydrolysis in most cases (Pape et al., 2005; Figure 1(b)). The latter compounds, however, can be biosynthesized by bacteria (Rütters et al., 2001) as well as animals such as fish (Hallgren and Larsson, 1962), sponge (Quijano et al., 1994), abyssal holothurians (Santos et al., 2002), corals (Imbs et al., 2006), etc. This may complicate the interpretation of biological source for MAGEs particularly in marine environments. Indeed, Hernandez-Sanchez et al. (2014) attributed different MAGEs distribution for marine water column and sediments, respectively, to mutiple microbial sources.

Compared to marine realms, MAGEs in terrestrial and other aquatic environments are less studied, thereby hindering our comprehensive understanding of their biological sources and subsequently of the biogeochemical roles of their precursors. Here we investigated the MAGEs distribution in surface soils across large environmental gradients (varied pH and climate), lake sediments and cave deposits. Given that lipid distribution pattern can generally provide important information about the microbial community structures and associated environmental change, MAGE distribution in these terrestrial settings was compared with those in previously reported bacterial pure cultures and marine environments to determine whether MAGEs in varied environments share the same sources.

1 Materials and methods

1.1 Sample collection and preparation

Thirty-four surface soil samples were collected from different climatic zones of China. Thirty-three samples of them have been used for GDGTs analysis by Yang et al. (2014b) (Figure 2). The detailed sample information is presented in Table 1. Soil samples were wrapped in the aluminum foil and kept in paper envelopes. Upon arrival at the laboratory, the samples were stored at –20°C refrigerator. The soils were then freeze dried and ground into powder with a pestle

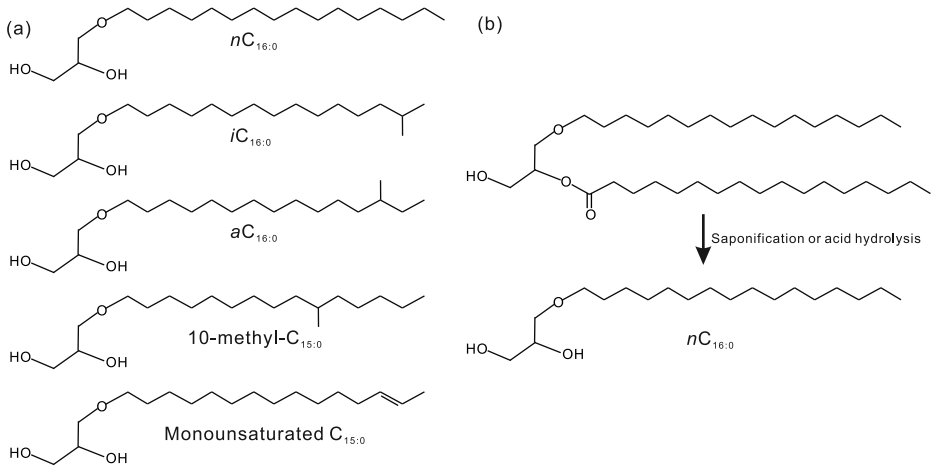

Figure 1 The structures of selected 1-*O*-monoalkyl glycerol ethers (a) and the transformation of 1-*O*-alkyl-2-acyl-3-*sn*-glycerol to 1-*O*-monoalkyl glycerol ether by base or acid hydrolysis (b).

Table 1 Sample information for lake sediments, soils, and cave deposits

No.	Samples	Sample type	MAT (°C)	pH	MAP (mm)	Latitude (N)	Longitude (E)	Altitude (m)	Depth
1	QHL-5	Lake sediment	0.5	9.08	391.9	n.a.[a)]	n.a.	3197	n.a.
2	QhL-7	Lake sediment	0.5	8.77	391.9	37°00′	100°01′	3197	25 m water depth
3	QHL-9	Lake sediment	0.5	8.13	391.9	37°00′	100°01′	3197	0.5 m water depth
4	Qhi-11	Lake sediment	0.5	8.56	391.9	36°44′	99°49′	3197	5 m water depth
5	Lzi-L-6	Lake sediment	17.1	8.16	1269.0	30°14.4′	114°36.2′	16	1.6 m water depth
6	Lzi-L-26	Lake sediment	17.1	8.12	1269.0	30°13.2′	114°36.1′	16	2.2 m water depth
7	Lzi-L-29	Lake sediment	17.1	8.19	1269.0	30°12.4′	114°34.6′	16	2.2 m water depth
8	Lzi-L-12	Lake sediment	17.1	7.70	1269.0	30°16.0′	114°34.8′	16	3 m water depth
9	WAL-16	Lake sediment	17.1	6.90	1269.0	30°35′	114°32′	20	n.a.
10	WAL-4	Lake sediment	17.1	6.89	1269.0	30°33′	114°31′	18	1.4 m water depth
11	WAL-14	Lake sediment	17.1	7.26	1269.0	30°32′	114°22′	20	3.7 m water depth
12	WAL-17	Lake sediment	17.1	7.12	1269.0	30°32′	114°22′	20	3.7 m water depth
13	LP-22	Soil	9.0	9.90	428.8	37°34.3′	110°30.7′	1001	Surface soil
14	PJ-6	Soil	9.5	8.49	643.4	n.a.	n.a.	6	0–10 cm
15	LP-34	Soil	10.6	6.93	582.5	35°13.4′	109° 2.1′	1098	Surface soil
16	XYB-2	Soil	11.4	7.76	924	33°33.8′	108°36.0′	1037	Surface soil
17	XJBC-5	Soil	12.1	8.41	61.1	39°45.1′	78°31.3′	1116	0–12 cm
18	Salt pool	Soil	8.3	9.14	273.5	37°45.9′	107°25.7′	1293	Surface soil
19	CD-5	Soil	16.1	7.46	870.1	30°40.9′	103°49.2′	530	0–5 cm
20	CD-7	Soil	16.1	7.38	870.1	30°40.9′	103°49.2′	530	0–5 cm
21	DYLJ-1	Soil	12.6	8.69	568.5	37°29.6′	118° 15.3′	9	Surface soil
22	DYLJ-3	Soil	12.6	8.40	568.5	37°29.6′	118° 15.3′	9	Surface soil
23	SNJ 3-1	Soil	1.4	5.94	n.a.	31°27.0′	110°16.0′	2840.00	0–7 cm
24	DHS-6	Soil	20.8	3.50	1956	23°10.2′	112°32.8′	100	0–10 cm
25	DHS-7	Soil	20.8	4.18	1956	23°10.1′	112°32.9′	44	0–10 cm
26	HS-S-2	Soil	16.8	7.78	1138	30°27.0′	110° 25.2′	ca. 294	Surface soil
27	HS4-11	Soil	16.8	7.95	1138	30°27.0′	110° 25.2′	ca. 294	Surface soil
28	2009-5-31	Soil	16.6	5.10	1269	30°31.5′	114° 24.3′	64	Surface soil
29	2009-1-13	Soil	17.1	n.a.	1269	30°31.5′	114° 24.3′	64	Surface soil
30	WH2009	Soil	17.1	5.11	1269	30°31.5′	114° 24.3′	64	0–2 cm
31	XZ-49	Soil	8.0	7.18	426.4	29°39.6′	90°55.7′	3696	Surface soil
32	XZ-23	Soil	8.2	6.34	641	29°45.9′	94°44.3′	3351	Surface soil
33	10NJ-S-2	Soil	13.7	8.17	553.3	34°21.0′	109°32.0′	637	0–5 cm
34	JFL-1-1	Soil	16.1	4.69	n.a.	18°43.0′	108°52.2′	1405	0–ca.10 cm
35	JFL-2b-1	Soil	16.7	4.40	n.a.	18°43.0′	108°52.5′	1296	0–ca.10 cm
36	JFL-4b-1	Soil	17.7	4.49	n.a.	18°42.8′	108°52.5′	1137	0–ca.10 cm
37	JFL-5a-1	Soil	18.6	4.18	n.a.	18°42.7′	108°52.6′	1002	0–ca.10 cm
38	JFL-6a-1	Soil	19.2	4.40	n.a.	18°42.3′	108°52.3′	899	0–ca.10 cm
39	JFL-7a-1	Soil	19.9	4.24	n.a.	18°42.2′	108°52.1′	790	0–ca.10 cm
40	JFL-8b-1	Soil	20.4	4.35	n.a.	18°41.8′	108°51.3′	701	0–ca.10 cm
41	JFL-9a-1	Soil	21.4	4.24	n.a.	18°42.0′	108°51.1′	597	0–ca.10 cm
42	JFL-10a-1	Soil	21.7	4.03	n.a.	18°42.0′	108°50.5′	497	0–ca.10 cm
43	JFL-11-1	Soil	22.3	4.81	n.a.	18°42.1′	108°50.2′	402	0–ca.10 cm
44	JFL-12-1	Soil	23.0	4.38	n.a.	18°41.9′	108°49.9′	290	0–ca.10 cm
45	JFL-13-1	Soil	23.5	5.89	n.a.	18°42.1′	108°49.7′	199	0–ca.10 cm
46	JFL-14-1	Soil	24.2	6.20	n.a.	18°42.2′	108°47.4′	86	0–ca.10 cm
47	Lotus Down	Cave deposit	16.8	n.a.	1138	30°27.0′	110°25.2′	ca. 294	Surface sediment
48	Rock-surf	Cave deposit	16.8	n.a.	1138	30°27.0′	110°25.2′	ca. 294	Surface sediment

a) n.a.: not available.

and mortar. The mean annual air temperature (MAT) for the sampling sites varies from 1.4 to 24.2°C and mean annual precipitation (MAP) from 61.1 to 1956 mm. The soil pH was measured following Yang et al. (2011). Briefly, soil powder was mixed with ultrapure water in a ratio of 1:2.5 (g/mL) and allowed to stand for 30 min. The supernatant was measured with a pH meter (×3) and final pH result was the average of three replicates.

A total of eight surface sediments were collected using a grabber from five fresh water lakes around Wuhan, the capital city of Hubei Province in Central China (Figure 2). Additionally, four surface sediments from the Lake Qinghai, a

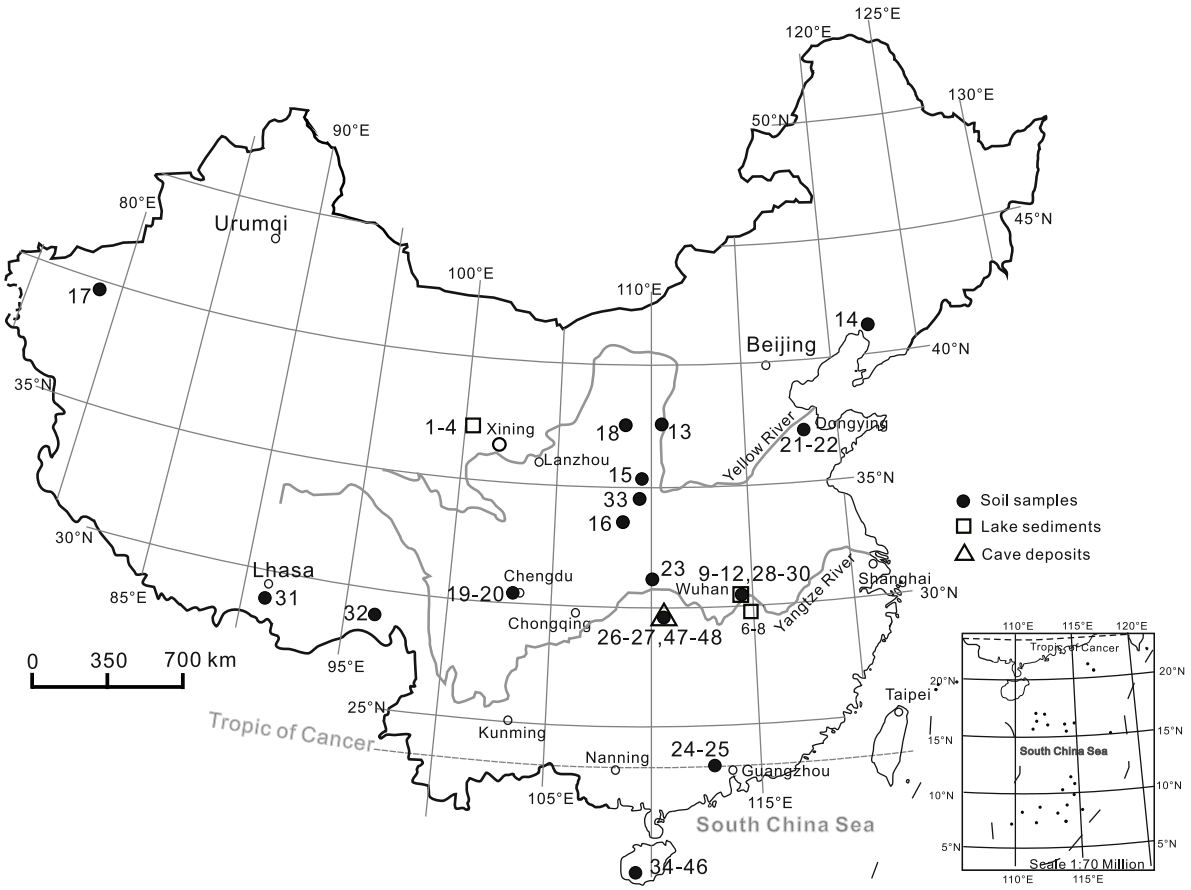

Figure 2 Sampling sites for surface soils, lake sediments, and cave deposits.

saline lake on the Qinghai-Tibetan Plateau were also sampled to make comparison with those fresh water lakes (Table 1). Sediments were transported to laboratory immediately and freeze dried. The dried samples were homogenized and ground into powder with a pestle and mortar. The MAT for Wuhan and Lake Qinghai are 17.1°C and –0.3°C, and MAP for them 1269 mm and 381.3 mm, respectively. The pH for lake sediments are measured following the methods for soils. The lakes around Wuhan are subjected to a typical East Asian monsoon climate, whereas the Lake Qinghai is situated at the boundary of Asian summer monsoon.

Two cave carbonate deposits were collected in the Heshang Cave of Hubei Province, China (Figure 2). Carbonate samples were scraped from the surface of a growing stalagmite and a collapsed dolomite, respectively, using a steel shovel. These samples were also ground into powder for further analysis. The MAT and MAP outside the Heshang cave (from 1971 to 2000) are 16.8°C and 1138 mm, respectively.

1.2 Lipid extraction and fractionation

An aliquot of each sample including soil, lake sediments and cave deposit was extracted (×6) ultrasonically with a mixture of dichloromethane (DCM) and methanol (MeOH) (9∶1, v/v). The supernatant was collected and combined to yield total lipid extraction (TLE) after the mixture was centrifuged. The TLE was concentrated in a rotary evaporator and dried under a gentle nitrogen gas. The TLE was then subjected to saponification by 2 N KOH/MeOH solutions (5% H_2O) at 80°C. The resulting solution was extracted with hexane (×6), yielding the neutral fraction containing MAGEs and alkanols. The neutral fraction was then separated into alkanes and polar fractions. Preganol was added to polar fraction as the internal standard. The polar fraction was silylated with BSTFA (70°C, 1.5 h) to convert alcohols into trimethylsilyl derivatives.

1.3 GC-MS analysis

The derivatised alcohols were analyzed by an Agilent 7890 gas chromatography and 5975 mass spectrometer (GC-MS) equipped with a silica capillary column (DB-5MS; 60 m× 0.25 mm×0.25 μm). The GC and MS conditions were as follows. The GC oven temperature ramped from 70 to 230°C at 3°C/min, and then from 230 to 300°C at 2°C/min, held at 300°C for 20 min with helium as the carrier gas. The inlet temperature was 300°C and the injection volume was 1 μL. The ionization energy was 70 eV and the temperature of

interface between GC and MS was set as 280°C. The normal, *iso*- and *anteiso*-MAGE were denoted, respectively, by nC$_{x:y}$, iC$_{x:y}$ and aC$_{x:y}$, where x represents the carbon number before derivatisation and y means the number of double bonds. The prefix "Me" or "*m*" represents middle-chain methyl branching.

2 Results and discussion

2.1 Identification of MAGEs

A variety of MAGEs detected in all samples were identified based on the characteristic fragment ions in the mass spectra and the relative elution order. The glycerol moiety of MAGEs has the *sn*-1,2 configuration, and MAGEs in the environmental samples have been proposed to be of a bacterial origin in a number of previous studies (Pancost et al., 2005; Oppermann et al., 2010). All the mass spectra of MAGEs show a typical *m*/*z* 205 fragment ion at the base peak, consistent with the cleavage between the *sn*-1 and *sn*-2 position of glycerol moiety and the assignment of the stereostructure of glycerol moiety (Figure 3(a) and (b)). The molecular ions ($M^{+\cdot}$) for saturated MAGEs are generally absent in the spectra as they readily lose a methyl moiety and consequently yield a $[M\text{-}15]^+$ ion that can be used to determine the molecular weight of related MAGEs. In contrast, both of the molecular and $[M\text{-}15]^+$ ions of monounsaturated MAGEs (e.g., nC$_{16:1}$) are apparent and 2 Da less than their saturated counterparts, with higher abundance of the former than the latter (Figure 3(b)). Useful fragment ions for determination of molecular weight also include $[M\text{-}90]^{+\cdot}$, $[M\text{-}103]^+$ and $[M\text{-}147]^{+\cdot}$, which represents the loss of one $HOSi(CH_3)_3$ moiety, an additional methylene (CH_2) moiety from the former $[M\text{-}90]^{+\cdot}$ fragment and two $Si(CH_3)_3$ moieties, respectively. The above diagnostic fragment ions allow identifying a series of MAGE homologs with carbon

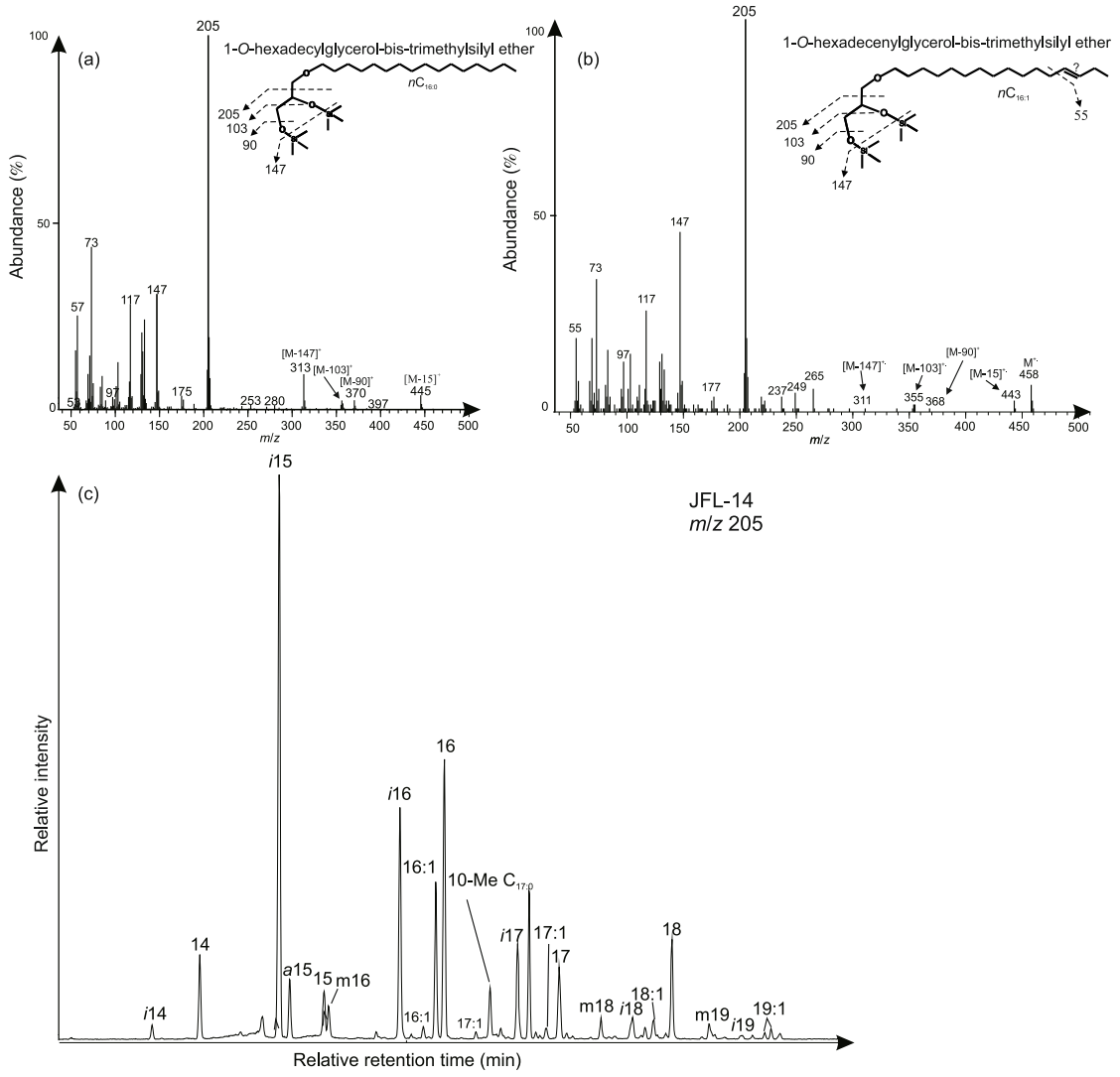

Figure 3 Examples showing the diagnostic fragment ions of normal (a), tentatively assigned monounsaturated MAGEs (b), and the elution orders of MAGE isomers (c) in the gas chromatogram.

number ranging from 14 to 22 in soils, lake sediments, and cave deposits.

Identification of MAGE isomers with different methyl positions relies largely on the elution order and published literatures (Oppermann et al., 2010) as these isomers have similar mass spectra to their corresponding normal MAGEs. The branched MAGEs generally have lower boiling points than their normal and monounsaturated counterparts, and hence the former elutes earlier in the gas chromatogram than the latter. This is similar to other branched lipid biomarkers (e.g., fatty acids and alcohols), which show an earlier elution time than their normal isomers as well as unsaturated counterparts (Yang et al., 2014c). In general, *iso*-MAGE elutes first, closely followed by *anteiso*-MAGEs and then the unsaturated MAGEs, whereas isomers with methyl group at middle position (Me-MAGE) elute before *iso*-MAGEs (Figure 3(c)). We did not perform the dimethyldisulfur derivatisation on the fatty alcohols and, therefore, the monounsaturated MAGEs are tentatively assigned. The tentatively assigned double bond of $n\mathrm{C}_{16:1}$ is perhaps located at either ω-1 or -2, or -3 positions because *m*/*z* 55 reveals there is an unsaturated bond in this fragment ion. The similar time interval between two adjacent *iso*-, *anteiso*- or normal MAGE homologs can also aid in the assignment of MAGEs isomers.

2.2 MAGEs in surface soils

The branched, monounsaturated and saturated MAGEs can be found in all the surface soil samples. As these soils were formed in considerably different climatic conditions, the ubiquitous occurrence of MAGEs in soils reveals that the precursor bacteria can tolerate a large soil pH range from 3.5 to 9.9. The carbon number of MAGEs generally ranges from C_{14} to C_{20} (Figure 4(a)), whereas $n\mathrm{C}_{21}$ and $n\mathrm{C}_{22}$-MAGE can be detected in some samples, e.g., JFL-11. Unlike the marine realms where $n\mathrm{C}_{12:0}$-MAGE and $n\mathrm{C}_{13:0}$-MAGE are apparent (Hernandez-Sanchez et al., 2014), MAGEs with carbon number $<\mathrm{C}_{14}$ are below the detection limit in all the soils analyzed (Table 2). The concentration (normalized to TOC) of total MAGEs varies from 0.12 to 13.2 μg g^{-1} TOC. The average MAGE concentrations for soil at pH > 7 and pH < 7, respectively, do not show a significant difference ($P > 0.05$, independent-sample *t*-test by SPSS software), indicating the MAGE-producing bacteria might have no obvious preference for soil pH. The $i\mathrm{C}_{15:0}$ component generally dominates the MAGE profile, followed by $n\mathrm{C}_{16:0}$, $i\mathrm{C}_{16:0}$ and $n\mathrm{C}_{16:1}$. The large structural diversity in branched MAGEs, including *iso*/*anteiso* MAGEs as well as MAGEs with methyl moiety at the middle position indicates MAGEs are primarily of a bacterial origin in soils. The $n\mathrm{C}_{17:0}$-MAGE generally has more than 3 isomers with different methyl position, similar to the fatty acids and alcohols in a given sample (Yang et al., 2014c). The branched MAGEs including $m\mathrm{C}_{16:0}$, $m\mathrm{C}_{18:0}$ and $m\mathrm{C}_{19:0}$ occur in these soils, whereas their fatty acids and alcohols counterparts are generally absent.

The overall distribution of MAGEs in all these soils does not change significantly with any given environmental variable including MAT, MAP, and soil pH. However, we observe that the ratio of $i\mathrm{C}_{15:0}/a\mathrm{C}_{15:0}$ shows a significant logarithmic relationship with soil pH ($R^2 = 0.62$, $P < 0.001$). The pH essentially represents the logarithm of proton concentration and the proton gradient across the cell membrane depends primarily on the proton concentration outside the cell. Hence, we employ the logarithm of $i\mathrm{C}_{15:0}/a\mathrm{C}_{15:0}$ ratio and find it shows a negative linear correlation with soil pH ($R^2 = 0.62$, $P < 0.001$; Figure 5). Specifically, the abundance of $i\mathrm{C}_{15:0}$-MAGE relative to $a\mathrm{C}_{15:0}$ decreases with soil pH. This is most likely to be the result of adaptation of microbial membrane composition to proton gradient in soils. In fact, the decrease in the abundance of $i\mathrm{C}_{17:0}$-MAGE relative to $a\mathrm{C}_{17:0}$ with pH can also be observed in these soils.

2.3 Distribution of MAGEs in lake sediments

A large diversity of branched, saturated, and monounsaturated MAGEs can be found in both the Qinghai Lake and the freshwater lake around Wuhan. The carbon number of MAGE in the lakes ranges from 14 to 22 (Figure 4(c)) and the summed concentration of total MAGEs varies from 0.76 to 458.8 μg g^{-1} TOC (Table 2). Almost all the lake sediments show a similar MAGE distributional pattern dominated by $n\mathrm{C}_{16:0}$. Most of the samples are also characterized by high abundance of 10-Me-$\mathrm{C}_{16:0}$, $n\mathrm{C}_{18:0}$ or $a\mathrm{C}_{15:0}$. In three samples (WAL-4, QHL-9, QHL-11), $i\mathrm{C}_{15:0}$ accounts for 20%, 37%, and 20% of total MAGEs, respectively, which closely resembles the MAGE distribution in soils. In both QHL-7 and QHL-11, $a\mathrm{C}_{15:0}$ exceed $i\mathrm{C}_{15:0}$ in abundance whereas other lake samples have higher abundance of $i\mathrm{C}_{15:0}$ than $a\mathrm{C}_{15:0}$. The ratio of $i\mathrm{C}_{15:0}/a\mathrm{C}_{15:0}$ for lake sediments varies from 0.58 to 6.43, which is significantly smaller than that for soils (2.5–36.2; independent-sample *t*-test by SPSS software, $F = 7.36$, $P < 0.05$, Figure 6).

The MAGE distributional difference between soils and lake sediments can also be reflected by the ratio of $i\mathrm{C}_{15:0}/n\mathrm{C}_{16:0}$, which is significantly higher in soils than in lake sediments (Figure 6). This difference indicates that there is in situ production of MAGEs in the lake environment, though contribution of MAGEs from catchment soils cannot be fully excluded. The pH and temperature variation cannot explain the considerable difference in MAGE distribution between lake sediments and soils. Although MAT and soil pH span large ranges across the climatic transect in this study, the dominance of $i\mathrm{C}_{15:0}$-MAGE followed by $n\mathrm{C}_{16:0}$ is not changed throughout the soil samples. Similarly, climatic parameters are not likely to impact on the MAGE distribution in lake sediments where $n\mathrm{C}_{16:0}$-MAGE generally dominates. Therefore, the different MAGE assemblages between aquatic and soil environment are likely to be the result of

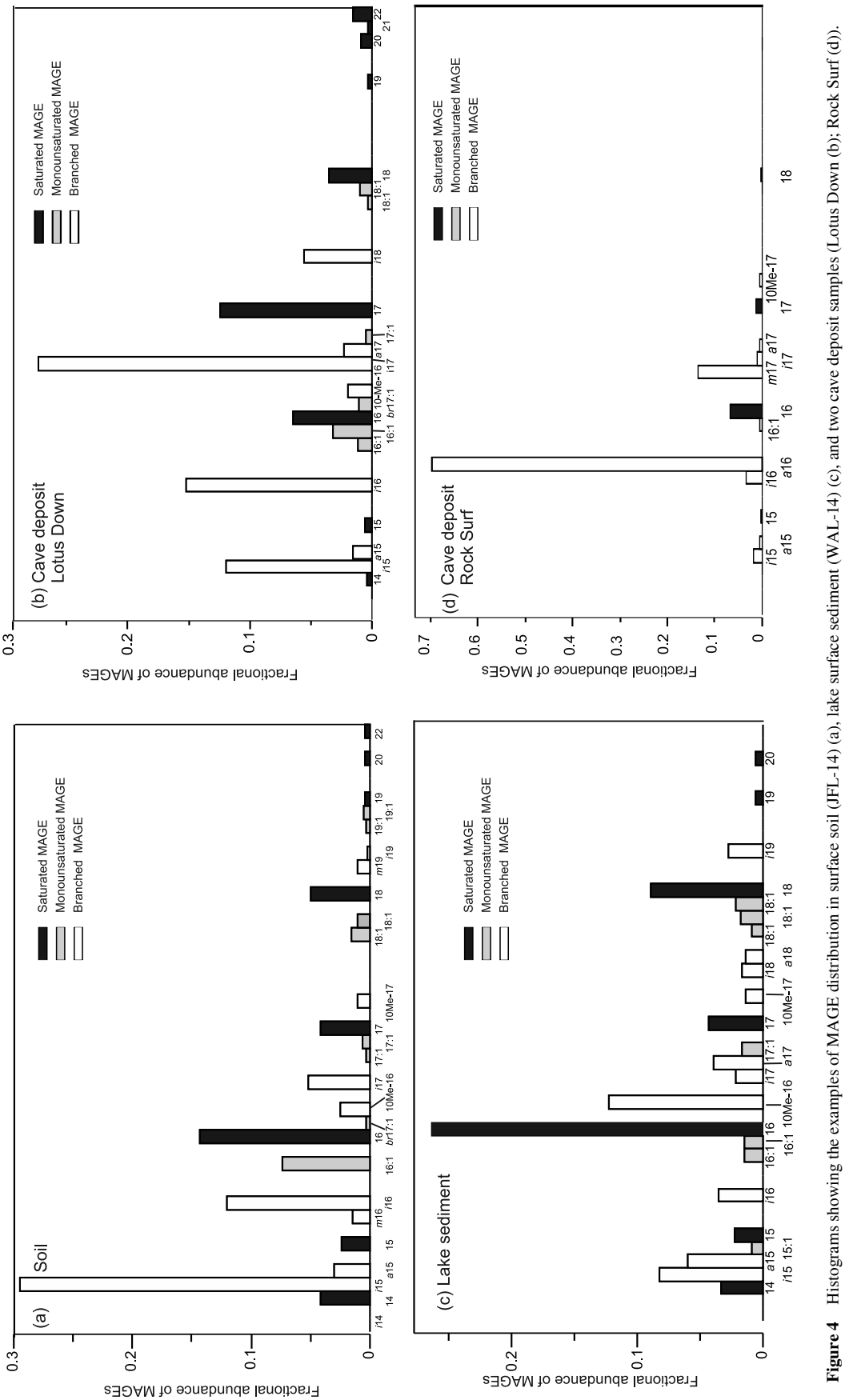

Figure 4 Histograms showing the examples of MAGE distribution in surface soil (JFL-14) (a), lake surface sediment (WAL-14) (c), and two cave deposit samples (Lotus Down (b); Rock Surf (d)).

Table 2 Fractional abundances of major MAGEs (normalized to total MAGEs for each sample) for lake sediment, soil, and cave deposit

	14	*i*15	*a*15	15	*i*16	16:1	16	10-Me-16	*i*17	17	18:1	18:1	18
QHL-5	0.04	0.10	0.04	0.05	0.03	0.04	0.36	0.05	0.03	0.03	0.00	0.07	0.05
QhL-7	0.03	0.06	0.11	0.04	0.07	0.03	0.27	0.07	0.03	0.03	0.02	0.06	0.05
QHL-9	0.00	0.37	0.10	0.00	0.00	0.00	0.38	0.00	0.00	0.00	0.00	0.00	0.00
Qhi-11	0.00	0.20	0.30	0.00	0.00	0.00	0.51	0.00	0.00	0.00	0.00	0.00	0.00
Lzi-L-6	0.02	0.07	0.04	0.03	0.03	0.02	0.29	0.13	0.03	0.06	0.01	0.02	0.07
Lzi-L-26	0.02	0.08	0.06	0.05	0.03	0.02	0.29	0.08	0.03	0.05	0.02	0.02	0.09
Lzi-L-29	0.01	0.05	0.04	0.03	0.03	0.01	0.31	0.12	0.02	0.05	0.01	0.01	0.08
Lzi-L-12	0.02	0.08	0.05	0.03	0.04	0.02	0.28	0.13	0.03	0.06	0.02	0.00	0.06
WAL-16	0.04	0.11	0.04	0.04	0.03	0.01	0.39	0.06	0.02	0.05	0.01	0.01	0.07
WAL-4	0.04	0.20	0.03	0.09	0.04	0.01	0.23	0.04	0.07	0.02	0.00	0.01	0.04
WAL-14	0.04	0.09	0.06	0.02	0.03	0.02	0.27	0.10	0.03	0.05	0.01	0.02	0.10
WAL-17	0.03	0.08	0.06	0.02	0.04	0.01	0.26	0.12	0.02	0.04	0.01	0.02	0.09
LP-22	0.02	0.23	0.03	0.04	0.06	0.06	0.17	0.00	0.04	0.02	0.00	0.04	0.05
PJ-6	0.04	0.17	0.04	0.03	0.03	0.03	0.23	0.05	0.04	0.03	0.02	0.01	0.08
LP-34	0.02	0.18	0.03	0.03	0.05	0.03	0.09	0.04	0.04	0.07	0.00	0.05	0.08
XYB-2	0.03	0.21	0.03	0.03	0.07	0.03	0.14	0.02	0.05	0.04	0.03	0.04	0.06
XJBC-5	0.02	0.22	0.06	0.01	0.07	0.01	0.15	0.09	0.04	0.00	0.00	0.00	0.02
Salt pool	0.01	0.06	0.01	0.00	0.01	0.02	0.15	0.02	0.02	0.05	0.00	0.01	0.02
CD-5	0.05	0.30	0.02	0.02	0.04	0.00	0.16	0.03	0.05	0.03	0.00	0.00	0.08
CD-7	0.05	0.27	0.02	0.03	0.04	0.02	0.22	0.02	0.03	0.02	0.02	0.01	0.06
DYLJ-1	0.05	0.29	0.04	0.02	0.04	0.00	0.22	0.03	0.04	0.02	0.00	0.03	0.05
DYLJ-3	0.03	0.33	0.13	0.03	0.06	0.02	0.18	0.01	0.02	0.01	0.00	0.00	0.03
SNJ 3-1	0.03	0.34	0.05	0.02	0.04	0.02	0.15	0.10	0.04	0.05	0.00	0.00	0.02
DHS-6	0.02	0.16	0.01	0.04	0.12	0.00	0.22	0.13	0.05	0.03	0.00	0.01	0.04
DHS-7	0.03	0.26	0.01	0.02	0.05	0.05	0.20	0.10	0.07	0.05	0.00	0.00	0.08
HS-S-2	0.02	0.13	0.02	0.03	0.17	0.01	0.10	0.02	0.03	0.05	0.01	0.01	0.03
HS4-11	0.02	0.16	0.02	0.03	0.16	0.01	0.14	0.02	0.03	0.06	0.00	0.01	0.08
2009-5-31	0.03	0.29	0.03	0.04	0.25	0.00	0.16	0.03	0.04	0.03	0.00	0.00	0.03
2009-1-13	0.02	0.39	0.03	0.02	0.07	0.00	0.08	0.05	0.06	0.08	0.01	0.00	0.02
WH 2009-2	0.04	0.35	0.03	0.04	0.17	0.10	0.10	0.04	0.03	0.02	0.00	0.00	0.02
XZ-49	0.01	0.16	0.04	0.04	0.06	0.02	0.21	0.07	0.04	0.08	0.00	0.03	0.07
XZ-23	0.03	0.35	0.03	0.03	0.05	0.01	0.18	0.03	0.04	0.02	0.00	0.00	0.03
10NJ-S-2	0.03	0.23	0.03	0.03	0.18	0.00	0.16	0.00	0.02	0.04	0.00	0.00	0.04
JFL-1-1	0.02	0.23	0.02	0.02	0.22	0.06	0.18	0.05	0.04	0.06	0.01	0.01	0.03
JFL-2b-1	0.02	0.25	0.00	0.02	0.11	0.15	0.21	0.02	0.03	0.08	0.01	0.02	0.04
JFL-4b-1	0.01	0.21	0.01	0.02	0.18	0.04	0.19	0.05	0.10	0.08	0.01	0.00	0.03
JFL-5a-1	0.01	0.21	0.00	0.00	0.17	0.02	0.18	0.14	0.11	0.09	0.00	0.00	0.05
JFL-6a-1	0.02	0.26	0.01	0.02	0.13	0.03	0.23	0.07	0.06	0.05	0.00	0.00	0.06
JFL-7a-1	0.03	0.29	0.01	0.02	0.04	0.08	0.30	0.02	0.04	0.03	0.02	0.01	0.05
JFL-8b-1	0.02	0.27	0.02	0.02	0.06	0.00	0.28	0.03	0.04	0.04	0.01	0.02	0.07
JFL-9a-1	0.03	0.42	0.02	0.03	0.07	0.06	0.20	0.01	0.04	0.03	0.01	0.01	0.03
JFL-10a-1	0.02	0.26	0.02	0.03	0.13	0.04	0.16	0.04	0.09	0.08	0.02	0.01	0.05
JFL-11-1	0.02	0.28	0.03	0.02	0.10	0.04	0.16	0.05	0.06	0.06	0.01	0.01	0.07
JFL-12-1	0.02	0.22	0.01	0.02	0.12	0.04	0.20	0.04	0.09	0.08	0.02	0.01	0.06
JFL-13-1	0.03	0.35	0.03	0.03	0.12	0.07	0.12	0.03	0.05	0.05	0.00	0.01	0.04
JFL-14-1	0.04	0.29	0.03	0.02	0.12	0.07	0.14	0.03	0.05	0.04	0.02	0.01	0.05
Lotus Down	0.00	0.12	0.02	0.01	0.15	0.01	0.06	0.02	0.27	0.12	0.00	0.00	0.04
Rock Surf	0.00	0.02	0.00	0.00	0.03	0.00	0.07	0.00	0.01	0.01	0.00	0.00	0.00

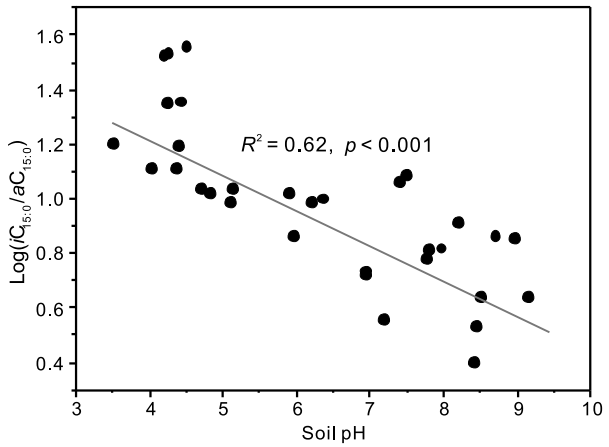

Figure 5 Cross plot showing a significant negative correlation between logarithm of $iC_{15:0}/aC_{15:0}$ ratio and soil pH.

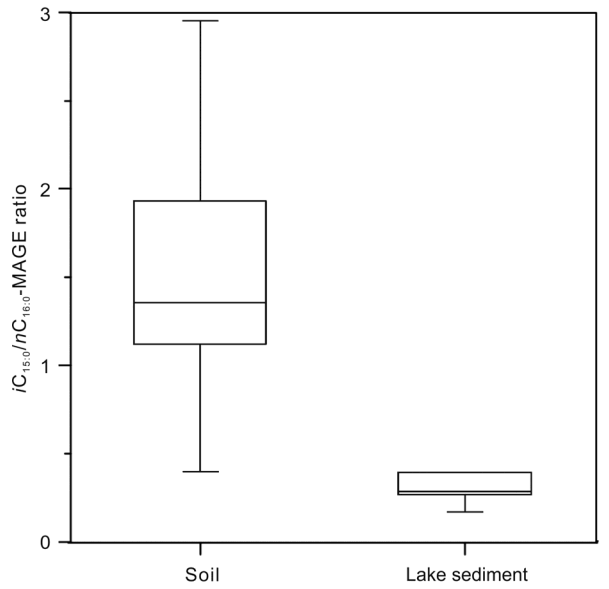

Figure 6 Box plot showing the range of $iC_{15:0}/nC_{16:0}$ ratio for soil and lake sediments. The boxplot shows minimum, maximum, median, lower quartile (25%), and upper quartile (75%) information for the ratio in different environments. An independent-sample *t*-test by SPSS software shows that the ratio of $iC_{15:0}/nC_{16:0}$ is statistically higher in soils than in the lakes ($F = 7.36$, $P < 0.05$).

changed bacterial communities.

The principal component analysis (PCA) on the fractional abundance of MAGEs in soils, and lake sediments clearly shows that samples from different environments cluster in different regions of the PCA plot (Figure 7), only except one lake sediment sample (WAL-4) that falls in the region of soils. This lake sediment has comparable abundance of $iC_{15:0}$ and $nC_{16:0}$ MAGEs, closely resembling that of soils. However, it has much higher abundance of $nC_{15:0}$ MAGE than other lake sediments and soils. As this lake is the shallowest (1.4 m) among all the fresh water lakes, the MAGE distribution in lake sediments is more likely to be influenced by the contribution from surrounding soils, resulting

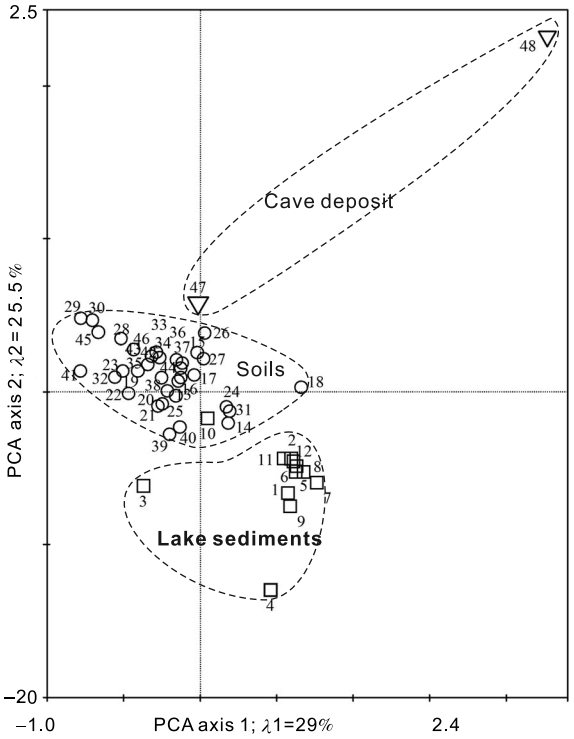

Figure 7 Principal component analysis (PCA) showing the clustering of different samples based on the fractional abundances of MAGEs. Note that a lake sediment sample, WAL-4, falls in the area for soils as its MAGE distribution closely resembles that for soils and might be impacted by soil organic input.

in a MAGE distribution more similar to soils than to other lake sediments. This is also true for a sample collected from the nearshore area of the Qinghai Lake, i.e., QHL-9, with a water depth of 0.5 m, shows approximate abundance of $iC_{15:0}$ and $nC_{16:0}$ MAGEs. The BIT value, a proxy reflecting the terrigenous organic input (Hopmans et al., 2004), for this sample is high (0.93, unpublished data), probably indicating a significant amount of soil organic matter input. Therefore, the autochthonous MAGEs in lake sediments are likely to be dominated by $nC_{16:0}$ MAGEs while increased abundance of $iC_{15:0}$ MAGEs in lake sediments may be indicative of enhanced soil organic input.

2.4 MAGEs distribution in cave deposit

The karst cave is a unique isolated subsurface environment where sunlight cannot readily reach and chemolithotrophic lifestyle generally dominates. Although cave deposit, e.g., stalagmite or sinter, may inherit organic matter from overlying soils, the archaeal and bacterial lipids in these deposits are thought to be both predominantly produced *in situ* in the cave (Yang et al., 2011; Blyth et al., 2014), based principally on the distinct GDGT distribution between soils overlying the caves and stalagmites. The two cave deposit samples (Rock Surf and Lotus Down) also show remarkably different MAGE distribution than soils overlying the cave

(HS-S-2 and HS4-11), although the carbon number for these samples also ranges from 14 to 22 (Table 2). The branched MAGEs including iC$_{17:0}$, iC$_{16:0}$ and iC$_{15:0}$ dominate in Lotus Down, a surface calcite sample from a growing stalagmite with iC$_{17:0}$ being the most abundant component (Figure 4(b)). The summed amount of branched MAGEs accounts for 84.2% of the total MAGE concentration in Lotus Down, which is much higher than that in HS-S-2 and HS4-11 (41.7% and 44.6%, respectively). Likewise, the dominant MAGEs in another cave deposit sample, Rock Surf, are also branched MAGEs, accounting for 91.1% of the total MAGEs. Specifically, aC$_{16:0}$ dominates in the MAGE profile, followed by mC$_{17:0}$ (Figure 4(d)) in this sample. As Rock Surf is less influenced by the dripping water and in turn the soil organic matter, the MAGEs for it are contributed primarily by the microbial mats residing on its surface. The dominance of MAGEs in the neutral lipid fraction of Rock Surf also highlights the importance of MAGE-producing bacteria in the microbial community. The autochthonous MAGEs in the cave obviously contrast with those in two overlying soils where MAGE distributions are dominated by iC$_{15:0}$ and iC$_{16:0}$, most likely pointing to a different bacterial source than soils.

2.5 Comparison of MAGEs distribution among environments and implication for their microbial sources

The previous knowledge about MAGEs has been generally related to phylogenetically deeply branching SRB or extremophiles (Hinrichs et al., 2000; Jahnke et al., 2001; Orphan et al., 2001; Rütters et al., 2001; Ge et al., 2011). A recent study of MAGE distribution in the particulate organic matter of water column and marine sediments reveals that some unknown aerobic bacteria other than SRB may also contribute significantly to the MAGE pool in marine realms (Hernandez-Sanchez et al., 2014). The ubiquitous occurrence of MAGEs in soils, lakes, and cave deposits in this study further expands our horizon about the habitats of MAGE-producing organism and also the sources of these orphan biomarkers.

The potential precursors of MAGEs in surface soils would be expected to at least have two characters, i.e., ubiquitous occurrence in soils and tolerance to oxygen exposure. The MAGEs in surface soils are not likely to be derived solely from the SRB for several reasons. Firstly, all the cultured SRB, e.g., *Desulfosarcina variabilis*, *Thermodesulfobacterium geofontis*, etc. (Table 3) do not produce a substantial amount of iC$_{15:0}$ that dominates in MAGE profiles for soils. They generally have nC$_{16:0}$-dominated MAGE pattern as observed in many cold seep sediments (Hinrichs et al., 2000). Secondly, the well-ventilated surface soils, particularly those dry soils from semiarid or arid regions, may not favor the anaerobic proliferation of mesophilic SRB. Instead, the abundant MAGEs in dry alkaline soils may point to aerobic microbial sources. In fact, *Myxcoccus xantus*, an aerobic bacteria found ubiquitously in soils, has been reported to biosynthesize iC$_{15:0}$-MAGE during formation of the fruiting body (Ring et al., 2006). This bacterium and its phylogenetic relatives are likely contributors of MAGEs in surface soils. Additionally, some cultured Acidobacteria species, e.g., *Acidobacteriaceae strain A2-4c* and *Pyrinomonas ethylaliphatogenes* falling into subdivisions 1 and 4 are also potential precursors of soil MAGEs as their lipids contain abundant iC$_{15:0}$-MAGE (Sinninghe Damsté et al., 2011; Crowe et al., 2014). The Acidobacteria subdivisions 1 and 4 are aerobic chemoorgantrophic bacteria. They have been found to be ubiquitous and abundant members of soil bacteria in diverse soils (Jones et al., 2009), indicating that they can potentially contribute considerable amount of iC$_{15:0}$ to soil MAGE pool. Nevertheless, as iC$_{15:0}$ and iC$_{17:0}$ were the only MAGEs found in the recently cultured Acidobacteria, other MAGEs including nC$_{16:0}$, nC$_{17:0}$, mC$_{17:0}$, and nC$_{18:0}$ etc. in surface soils are not likely to be of Acidobacteria origin. Hence, we speculate that the complex MAGE assemblages in soils are the results of bacteria falling into *Myxococcales* and *Acidobacteria* as well as other kinds of previously uncharacterized organisms.

The MAGE distribution pattern appears to be similar for different aquatic settings. Specifically, the nC$_{16:0}$-MAGE has been found to be dominant in lake sediments, cold seep sediments, marine surface sediments, particulate organic matter in marine water column and microbialites (Heindel et al., 2012; Hernandez-Sanchez et al., 2014). These water-saturated sedimentary environments facilitate the formation of anoxic micro-niches, which are conditions favorable to the production of widespread anaerobic SRB, *Aquifex* and *Firmicutes* (Langworthy et al., 1983; Langworthy and Pond, 1986; Huber et al., 1992; Huber et al., 1996; Rütters et al., 2001; Hamilton-Brehm et al., 2013) (Table 3). The SRB, as reflected by cultured mesophilic and thermophilic species (Table 3), are likely to be important contributors of nC$_{16:0}$-MAGE in lake sediments despite that these SRB are not necessarily the participants of AOM. The phylogenetic relatives of cultured *Firmicutes,* e.g., *Ammonifex degensii*, *Clostridium thermocellum*, etc. can contribute primarily iC$_{16:0}$, iC$_{15:0}$, and nC$_{16:0}$ as well as other relatively less abundant MAGEs with carbon number ranging from C$_{14}$ to C$_{18}$ to MAGE pool in lake sediments. The thermophilic *Aquifex* in the hot spring primarily produces MAGEs with longer chains (C$_{18}$–C$_{20}$) than other bacteria. These long-chain MAGEs are perhaps the diagnostic characters for *Aquifex* rather than the adaption of microbial membrane lipids to higher temperature because other MAGE-producing thermophilic bacteria like *Thermodesulfobacterium geofontis* do not produce any MAGE with carbon chain length >17. As mesophilic *Aquifex* is an important member of bacterial community in lakes, it is likely to be the source of long chain MAGEs (C >17) in the analyzed lake sediment samples.

The cave deposits, despite of only two samples, show

Table 3 Previously published MAGE distributions in cultured bacteria

Species	Isolated source	Phylogenetic affiliation	Culture condition	MAGEs	Dominant MAGEs	Reference
Thermodesulfotobacterium commune	Hot spring	SRB	Anaerobic, 45–85°C, pH 6.5–7	*br*$C_{17:0}$, *br*$C_{18:0}$, *n*$C_{18:0}$, *br*$C_{16:0}$, *br*$C_{19:0}$, *n*$C_{16:0}$	*a*$C_{17:0}$	Langworthy et al., 1983
Thermodesulfobacterium geofontis	Hot spring	SRB, *Thermodesulfobacteriaceae*	Anaerobic, 70–90°C, pH 6.5–7	*n*$C_{16:0}$, *i*$C_{16:0}$	*n*$C_{16:0}$, *i*$C_{16:0}$	Hamilton-Brehm et al., 2013
Desulfosarcina variabilis	n.a.[a)]	SRB, Proteobacteria	Anaerobic, 28–33°C	*n*$C_{16:0}$	*n*$C_{16:0}$	Rütters et al., 2001
Desulforhabdus amnigenus	Sludge	SRB, δ Proteobacteria	Anaerobic, 37°C	*n*$C_{15:0}$, *n*$C_{17:0}$	*n*$C_{15:0}$	Rütters et al., 2001
Aquifex	Hot spring	*Aquifex*	Anaerobic	$C_{18:1}$, C_{18}, C_{19}, $C_{20:1}$, C_{20}, $C_{21:1}$	C_{18}, C_{20}	Huber et al., 1992; Jahnke et al., 2001
Ammonifex degensii	n.a.	*Firmicutes*	n.a.	C_{14} to C_{18}	*n*$C_{16:0}$	Huber et al., 1996
Clostridium thermocellum	Cotton bale	*Firmicutes*	Anaerobic, 28–69°C, pH 6.1–7.5	*i*$C_{16:0}$, *n*$C_{16:0}$, *i*$C_{17:0}$	*n*$C_{16:0}$	Langworthy and Pond, 1986
C. thermosulfurogens	Hot spring	*Firmicutes*	Anaerobic, 35–75°C, pH 4–7.5	*i*$C_{15:0}$, *i*$C_{16:0}$	*i*$C_{16:0}$	Langworthy and Pond, 1986
C. thermohydrosulfuricum	n.a.	*Firmicutes*	Anaerobic, 65°C	*i*$C_{15:0}$	*i*$C_{15:0}$	Langworthy and Pond, 1986
Acidobacteriaceae strain A2-4c	Savanna soil	*Acidobacteria*	Aerobic	*i*$C_{15:0}$	*i*$C_{15:0}$	Sinninghe Damsté et al., 2011
Edaphobacter aggregans Wbg-1	Alpine soil	*Acidobacteria*	Aerobic, pH 4.5–7.0	*i*$C_{15:0}$	*i*$C_{15:0}$	Sinninghe Damsté et al., 2011
Pyrinomonas ethylaliphatogenes	Geothermally heated soil	*Acidobacteria*	Aerobic, 50–69°C, pH 4.1–7.8	*i*$C_{15:0}$, *i*$C_{17:0}$	*i*$C_{15:0}$, *i*$C_{17:0}$	Crowe et al., 2014
Myxcoccus xantus	Soil	*Myxococcales*	Aerobic	*i*$C_{15:0}$	*i*$C_{15:0}$	Ring et al., 2006

a) n.a.: not available.

completely different MAGE pattern than other environments. The dominance of $i\mathrm{C}_{17:0}$ and $a\mathrm{C}_{16:0}$, respectively in Lotus Down and Rock Surf, is not consistent with MAGE profile for any cultured bacterial species, likely pointing to other as-yet uncharacterized bacterial sources. This indicates that MAGEs, a suite of unique ether lipids, can be produced by more bacteria than ever expected. Although future genetic work is required, this initial survey on MAGEs in the terrestrial and aquatic environments highlights a variety of possible indicators. The ether lipids, due to their resistance to degradation, can be preserved in sediments over a relatively long geological time (Pancost et al., 2006; Saito et al., 2013). The potential of MAGEs as biomarkers for specific bacteria enables MAGE to be used to examine the past bacterial communities, which can further aid in interpreting the paleoenvironment. For example, MAGEs found in carbonate rocks and mud rocks deposited during the Early and Middle Triassic were likely derived from SRB, indicating that anoxic conditions might expand in the depositional and/or water column environment during that period (Pancost et al., 2006; Saito et al., 2013).

The ether lipids are generally believed to be more resistant to extremely acid, alkaline conditions or high temperature than acylglycerol lipids, because the addition of MAGEs may enhance the overall rigidity of cell membrane. Hence, more ether lipids can be found in hot spring environments where temperatures are generally high (Zeng et al., 1992a, 1992b; Pancost et al., 2005, 2006). However, the wide occurrence of MAGEs in mesophilic bacteria is apparently not an adaptation of their cell membrane to extreme environments. Instead, these mesophilic bacteria may inherit the nature of their extremophilic ancestors, which may biosynthesize a considerable amount of ether lipids to resist the extreme conditions. The MAGE-producing bacteria are capable of producing both ether and ester lipids, and they possess genes encoding the biosynthesis of both ether and ester lipids, which are common in Archaea and bacteria/Eukaryotes, respectively. Therefore, in terms of lipids, these MAGE-producing bacteria, including those uncharacterized, are likely to be the evolutionary intermediate between deeply branching microorganisms and non-extremophilic bacteria.

3 Conclusions

The MAGE distributions were investigated in the surface soils and lake sediments spanning large environmental gradients, and also in two typical cave deposit samples. These lipids, previously known as the biomarker of SRB mediating the AOM, were found ubiquitously in terrestrial and lake environments studied. This reveals that a great variety of bacteria can biosynthesize MAGEs and utility of MAGE as the biomarker for SRB is likely to be only limited to AOM environment. The three environments show distinctive MAGE distributions while the overall distribution pattern in either soil or lake sediments is generally consistent among samples. The MAGEs for surface soils are dominated by $i\mathrm{C}_{15:0}$, followed by $n\mathrm{C}_{16:0}$, as opposed to the dominance of $n\mathrm{C}_{16:0}$ over $i\mathrm{C}_{15:0}$ in lake sediments. This difference can be clearly reflected by the ratio of $i\mathrm{C}_{15:0}/n\mathrm{C}_{16:0}$. The higher values of this ratio in soils than in lake sediments, as well as other distributional difference between them, collectively suggest that MAGEs in lake sediments are likely to be produced in situ rather than contributed by catchment soils. The logarithm of the $i\mathrm{C}_{15:0}/a\mathrm{C}_{15:0}$ ratio for soil shows a significant negative correlation with soil pH, presumably reflecting an adaptation of cell membrane to proton concentration. The branched MAGEs are dominated in the two cave deposit samples, also pointing to different microbial sources than soils and lake sediments. The large diversity of MAGEs in soils, lake sediments, and cave deposits cannot be fully attributed to cultured bacterial species, suggesting MAGEs can be biosynthesized by more organisms than ever expected.

Two anonymous reviewers are thanked for their comments, which improved the original manuscript. We thank Yangming Qin for sampling soil and lake sediments and Xuan Qiu for GC-MS maintenance. This work was supported by the National Basic Research Program of China (Grant No. 2011CB808800), the National Natural Science Foundation of China (Grant No. 41330103) and the "111" Project (Grant No. B08030).

Blumenberg M, Seifert R, Reitner J, et al. 2004. Membrane lipid patterns typify distinct anaerobic methanotrophic consortia. Proc Natl Acad Sci USA, 101: 11111–11116

Blyth A J, Jex C N, Baker A, et al. 2014. Contrasting distributions of glycerol dialkyl glycerol tetraethers (GDGTs) in speleothems and associated soils. Org Geochem, 69: 1–10

Bradley A S, Fredricks H, Hinrichs K-U, et al. 2009. Structural diversity of diether lipids in carbonate chimneys at the Lost City Hydrothermal Field. Org Geochem, 40: 1169–1178

Crowe M A, Power J F, Morgan X C, et al. 2014. *Pyrinomonas methylaliphatogenes* gen. nov., sp. nov., a novel group 4 thermophilic member of the phylum Acidobacteria from geothermal soils. Int J Syst Evol Micr, 64: 220–227

Ge L, Jiang S, Yang T, et al. 2011. Glycerol ether biomarkers and their carbon isotopic compositions in a cold seep carbonate chimney from the Shenhu area, northern South China Sea. Chin Sci Bull, 56: 1700–1707

Hallgren B, Larsson S. 1962. The glyceryl ethers in the liver oils of elasmobranch fish. J Lipid Res, 3: 31–38

Hamilton-Brehm S, Gibson R, Green S, et al. 2013. *Thermodesulfobacterium geofontis* sp. nov., a hyperthermophilic, sulfate-reducing bacterium isolated from Obsidian Pool, Yellowstone National Park. Extremophiles, 17: 251–263

Heindel K, Birgel D, Brunner B, et al. 2012. Post-glacial microbialite formation in coral reefs of the Pacific, Atlantic, and Indian Oceans. Chem Geol, 304–305: 117–130

Hernandez-Sanchez M T, Homoky W B, Pancost R D. 2014. Occurrence of 1-*O*-monoalkyl glycerol ether lipids in ocean waters and sediments. Org Geochem, 66: 1–13

Hinrichs K U, Summons R E, Orphan V, et al. 2000. Molecular and isotopic analysis of anaerobic methane-oxidizing communities in marine sediments. Org Geochem, 31: 1685–1701

Hopmans E C, Weijers J W H, Schefu E, et al. 2004. A novel proxy for terrestrial organic matter in sediments based on branched and

isoprenoid tetraether lipids. Earth Planet Sci Lett, 224: 107–116
Huber R, Wilharm T, Huber D, et al. 1992. *Aquifex pyrophilus* gen. nov. sp. nov., represents a novel Group of marine hyperthermophilic hydrogen-oxidizing bacteria. Syst Appl Microbiol, 15: 340–351
Huber R, Rossnagel P, Woese C R, et al. 1996. Formation of ammonium from nitrate during chemolithoautotrophic growth of the extremely thermophilic bacterium *ammonifex degensii* gen. nov. sp. nov. Syst Appl Microbiol, 19: 40–49
Imbs A, Demina O, Demidkova D. 2006. Lipid class and fatty acid composition of the boreal soft coral *Gersemia rubiformis*. Lipids, 41: 721–725
Jahnke L L, Eder W, Huber R, et al. 2001. Signature lipids and stable carbon isotope analyses of Octopus spring hyperthermophilic communities compared with those of *Aquificales* representatives. Appl Environ Microb, 67: 5179–5189
Jenkyns H C, Schouten-Huibers L, Schouten S, et al. 2012. Warm Middle Jurassic-Early Cretaceous high-latitude sea-surface temperatures from the Southern Ocean. Clim Past, 8: 215–226
Jones R T, Robeson M S, Lauber C L, et al. 2009. A comprehensive survey of soil acidobacterial diversity using pyrosequencing and clone library analyses. ISME J, 3: 442–453
Langworthy T A, Holzer G, Zeikus J G, et al. 1983. Iso- and anteiso-branched glycerol diethers of the thermophilic anaerobe *Thermodesulfotobacterium commune*. Syst Appl Microbiol, 4: 1–17
Langworthy T A, Pond J L. 1986. Membranes and Lipids of Thermophiles, *Thermophilies:* General, Molecular and Applied Microbiology. New York: Wiley
Liu X L, Summons R E, Hinrichs K U. 2012. Extending the known range of glycerol ether lipids in the environment: structural assignments based on tandem mass spectral fragmentation patterns. Rapid Commun Mass Sp, 26: 2295–2302
Oppermann B I, Michaelis W, Blumenberg M, et al. 2010. Soil microbial community changes as a result of long-term exposure to a natural CO_2 vent. Geochim Cosmochim Acta, 74: 2697–2716
Orphan V J, Hinrichs K-U, Ussler W, et al. 2001. Comparative analysis of methane-oxidizing Archaea and sulfate-reducing bacteria in anoxic marine sediments. Appl Environ Microb, 67: 1922–1934
Pancost R D, Bouloubassi I, Aloisi G, et al. 2001. Three series of non-isoprenoidal dialkyl glycerol diethers in cold-seep carbonate crusts. Org Geochem, 32: 695–707
Pancost R D, Pressley S, Coleman J M, et al. 2005. Lipid biomolecules in silica sinters: indicators of microbial biodiversity. Environ Microbiol, 7: 66–77
Pancost R D, Pressley S, Coleman J M, et al. 2006. Composition and implications of diverse lipids in New Zealand Geothermal sinters. Geobiology, 4: 71–92
Pape T, Blumenberg M, Seifert R, et al. 2005. Lipid geochemistry of methane-seep-related Black Sea carbonates. Palaeogeogr Palaeoclimatol palaeoecol, 227: 31–47
Pearson E J, Juggins S, Talbot H M, et al. 2011. A lacustrine GDGT-temperature calibration from the Scandinavian Arctic to Antarctic: Renewed potential for the application of GDGT-paleothermometry in lakes. Geochim Cosmochim Acta, 75: 6225–6238
Quijano L, Cruz F, Navarrete I, et al. 1994. Alkyl glycerol monoethers in the marine sponge *Desmapsamma anchorata*. Lipids, 29: 731–734
Rütters H, Sass H, Cypionka H, et al. 2001. Monoalkyl ether phospholipids in the sulfate-reducing bacteria *Desulfosarcina variabilis* and *Desulforhabdus amnigenus*. Arch Microbiol, 176: 435–442
Řezanka T, Křesinová Z, Kolouchová I, et al. 2012. Lipidomic analysis of bacterial plasmalogens. Folia Microbiol, 57: 463–472
Ring M W, Schwar G, Thiel V, et al. 2006. Novel iso-branched ether lipids as specific markers of developmental sporulation in the Myxobacterium *Myxococcus xanthus*. J Biol Chem, 281: 36691–36700
Saito R, Oba M, Kaiho K, et al. 2013. Ether lipids from the Lower and Middle Triassic at Qingyan, Guizhou Province, Southern China. Org Geochem, 58: 27–42
Santos V L C S, Billett D S M, Wolff G A. 2002. 1-*O*-Alkylglyceryl ether lipids of the gut walls and contents of an abyssal Holothurian (*Oneirophanta mutabilis*). J Brazil Chem Soc, 13: 653–657
Schouten S, Hopmans E C, Pancost R D, et al. 2000. Widespread occurrence of structurally diverse tetraether membrane lipids: Evidence for the ubiquitous presence of low-temperature relatives of hyperthermophiles. Proc Natl Acad Sci USA, 97: 14421–14426
Schouten S, Hopmans E C, Schefuss E, et al. 2002. Distributional variations in marine crenarchaeotal membrane lipids: a new tool for reconstructing ancient sea water temperatures? Earth Planet Sci Lett, 204: 265–274
Sinninghe Damsté J S, Rijpstra W I C, Hopmans E C, et al. 2011. 13,16-Dimethyl octacosanedioic acid (*iso*-diabolic acid): A common membrane-spanning lipid of Acidobacteria subdivisions 1 and 3. Appl Environ Microbiol, 77: 4147–4154
Sinninghe Damsté J S, Rijpstra W I C, Strous M, et al. 2004. A mixed ladderane/n-alkyl glycerol diether membrane lipid in an anaerobic ammonium-oxidizing bacterium. Chem Commun: 2590–2591
Weijers J W H, Schouten S, Hopmans E C, et al. 2006a. Membrane lipids of mesophilic anaerobic bacteria thriving in peats have typical archaeal traits. Environ Microbiol, 8: 648–657
Weijers J W H, Schouten S, Spaargaren O C, et al. 2006b. Occurrence and distribution of tetraether membrane lipids in soils: Implications for the use of the TEX_{86} proxy and the BIT index. Org Geochem, 37: 1680–1693
Weijers J W H, Schouten S, Van Den Donker J C, et al. 2007. Environmental controls on bacterial tetraether membrane lipid distribution in soils. Geochim Cosmochim Acta, 71: 703–713
Yang H, Ding W, Zhang C L, et al. 2011. Occurrence of tetraether lipids in stalagmites: Implications for sources and GDGT-based proxies. Org Geochem, 42: 108–115
Yang H, Pancost R D, Tang C, et al. 2014a. Distributions of isoprenoid and branched glycerol dialkanol diethers in Chinese surface soils and a loess-paleosol sequence: Implications for the degradation of tetraether lipids. Org Geochem, 66: 70–79
Yang H, Pancost R D, Dang X, et al. 2014b. Correlations between microbial tetraether lipids and environmental variables in Chinese soils: Optimizing the paleo-reconstructions in semiarid and arid regions. Geochim Cosmochim Acta, 126: 49–69
Yang H, Pancost R D, Tang C, et al. 2014b. Distributions of isoprenoid and branched glycerol dialkanol diethers in Chinese surface soils and a loess–paleosol sequence: Implications for the degradation of tetraether lipids. Org Geochem, 66: 70–79
Yang H, Ding W, Xie S. 2014c. Distribution of microbial fatty acids and fatty alcohols in soils from an altitude transect of Mt. Jianfengling in Hainan, China: Implication for paleoaltimetry and paleotemperature reconstruction. Sci China Earth Sci, 57: 999–1012
Zeng Y B, Ward D M, Brassell S C, et al. 1992a. Biogeochemistry of hot spring environments: 3. Apolar and polar lipids in the biologically active layers of a cyanobacterial mat. Chem Geol, 95: 347–360
Zeng Y B, Ward D M, Brassell S C, et al. 1992b. Biogeochemistry of hot spring environments: 2. Lipid compositions of Yellowstone (Wyoming, U.S.A.) cyanobacterial and Chloroflexus mats. Chem Geol, 95: 327–345